

# The role of shell crossing on the existence and stability of trapped matter shells in spherical inhomogeneous $\Lambda$ -CDM models

Morgan Le Delliou\*  
*Instituto de Física Teórica UAM/CSIC,  
Facultad de Ciencias, C-XI,  
Universidad Autónoma de Madrid  
Cantoblanco, 28049 Madrid SPAIN*

Filipe C. Mena†  
*Centro de Matemática  
Universidade do Minho  
Campus de Gualtar, 4710-057 Braga, Portugal*

José P. Mimoso‡  
*Departamento de Física, Faculdade de Ciências da Universidade de Lisboa  
Centro de Astronomia e Astrofísica, Universidade de Lisboa,  
Campo Grande, Edifício C8 P-1749-016 Lisboa, Portugal*  
(Dated: Received...; Accepted...)

We analyse the dynamics of trapped matter shells in spherically symmetric inhomogeneous  $\Lambda$ -CDM models. The investigation uses a Generalised Lemaître-Tolman-Bondi description with initial conditions subject to the constraints of having spatially asymptotic cosmological expansion, initial Hubble-type flow and a regular initial density distribution. We discuss the effects of shell crossing and use a qualitative description of the local trapped matter shells to explore global properties of the models. Once shell crossing occurs, we find a splitting of the global shells separating expansion from collapse into, at most, two global shells: an inner and an outer limit trapped matter shell. In the case of expanding models, the outer limit trapped matter shell necessarily exists. We also study the role of shear in this process, compare our analysis with the Newtonian framework and give concrete examples using density profile models of structure formation in cosmology.

PACS numbers: 98.80.-k, 98.80.Cq, 98.80.Jk, 95.30.Sf, 04.40.Nr, 04.20.Jb

## I. INTRODUCTION

Studies of non-linear structure formation in cosmology, namely spherical top hat collapse models, often assume that there is no influence of the cosmological background on a finite domain which has disconnected from the background dynamics (see e.g. [1–4]).

We have looked at this problem in more detail in Ref. [5] and found local conditions under which such separation could be justified for inhomogeneous cosmological models. In particular, we have studied the possibility for perfect fluid solutions to exhibit locally defined separating shells between collapsing and the expanding (cosmological) regions.

The simplest examples given in [5] were set in an inhomogeneous universe of dust with a positive cosmological constant and the nature of the dust spherical shells allowed the system to be entirely determined from its initial conditions, at least, until the eventual occurrence of shell crossing.

However, shell crossings or caustics are expected to happen in these settings with more general initial conditions than in [5] and an interesting question is whether our previous results are robust with respect to the occurrence of shell crossing. This is the main concern in this paper, which can be regarded a natural follow up of our previous work [5].

Shell crossing in spherical symmetry has already been studied in several past works, although in contexts different from the one of present paper. For Lemaître-Tolman-Bondi (hereafter LTB) spacetimes shell crossing conditions were established by Hellaby and Lake [6] in terms of the metric data and more recently re-written by Sussman in terms of quasi-local scalars [8, 9]. Goncalves [10], has shown that shell crossing exists for  $\Lambda$ -LTB spacetimes with charge. In [11], it has been shown that shell-crossing occurs for a large class of initial conditions in models of formation of voids and some cases of fluids with pressure gradients.

There were also several works about the strength of shell crossing singularities, with the general conclusion that it is a weak singularity in the sense of Tipler [12]. This then raised the question of the continuity of the metric across these singularities and, very interestingly, solutions of dynamical extension through shell crossing singularities of LTB have been proved to exist, by Nolan [13], while the case including a cosmological constant and

---

\* Also at Centro de Física Teórica e Computacional, Universidade de Lisboa, Av. Gama Pinto 2, 1649-003 Lisboa, Portugal; Morgan.LeDelliou@uam.es, delliou@cii.fc.ul.pt

† fmena@math.uminho.pt

‡ jpmimoso@cii.fc.ul.pt

electric charges has been discussed by Gonçalves [10].

A complementary treatment was given by Nunez et al. [14] for metric extensions through shell crossing based on the interactions between shells, which translate in a conservation relation between mass and momenta, for timelike massive shells. Physically, this conservation relation summarises the microphysics of the fluid, however *for dust*, only purely gravitational interaction occurs between crossing shells, hence *the rest mass of each shell is conserved* [15].

Here, we shall not deal with the problem of metric extensions after shell crossing and, motivated by the above results, we shall assume the validity of the field equations in between shell crossing events and the continuity of the radial coordinates. Our main concern here will be to study the effects of shell crossing on the existence and stability of separating shells in spherical symmetry. In this paper, we shall also discuss the role of shear in the formation of shells which separate expanding from collapsing regions, we shall compare our results with Newtonian cases and give a concrete example of initial data which develops shell crossing and exhibits separating shells in a  $\Lambda$ -dust model.

The models considered in this paper obey the following properties: (a) spherically symmetric dust (the rest mass of infinitesimal pressureless shells is conserved under shell crossing) with a cosmological constant in Generalised LTB (GLTB) system ; (b) Lagrangian treatment of the radial coordinates (assume there are metric extensions through shell crossings); (c) asymptotic spatial cosmological behaviour (Friedmann-Lemaître-Robertson-Walker, hereafter FLRW, at spatial infinity); (d) initial Hubble-type flow (outgoing initial velocities); (e) regular initial density distribution (no finite mass for infinitely thin shell, and no singularity or zero density at the centre).

The paper is organized as follows: in a first part (II) we recall the conditions for the existence of matter trapped shells and study the role of shear on the existence of those shells in  $\Lambda$ -LTB models. Section (III) is devoted to the study of the effect of shell crossing in  $\Lambda$ -LTB models. In particular, we perform a dynamical analysis and separate this study into a local and global effects. We give concrete examples in section (IV) before presenting the final conclusions.

## II. TRAPPED MATTER SHELLS IN $\Lambda$ -CDM

### A. Conditions for the existence of trapped matter shells

In this section, we briefly recall some results of our previous paper [5] which did not consider shell-crossings.

The GLTB system proposed in Refs. [5, 16], has the following simple form for the case of a  $\Lambda$ -dust model where  $P' = 0$  and  $P = P_{dust} = 0$  (here we set  $G = 1 = c$ ,  $\Lambda > 0$ ,  $\alpha$  is the lapse function,  $r(T, R)$  the areal radius and  $E$

the energy of spatial hypersurfaces<sup>1</sup>)

$$ds^2 = -\alpha(t, R)^2 dt^2 + \frac{(\partial_R r)^2}{1 + E(t, R)} dR^2 + r^2 d\Omega^2. \quad (1)$$

The Bianchi identities projected along and orthogonal to the timelike flow  $n = \partial_t$  yield ( $P$  is the pressure,  $\rho$  the density, the prime  $'$  denotes  $\partial_R$ , a dot  $\dot{\phantom{x}}$  stands for  $\partial_t$  and  $\Theta$  is the expansion along the flow)

$$\dot{\rho} = -(\rho + P)^3 \Theta, \quad (2)$$

$$-\frac{P'}{\rho + P} = \frac{\alpha'}{\alpha} = 0 \Rightarrow \alpha dt = dt^* \Rightarrow \alpha = 1, \quad (3)$$

and the Einstein Field Equations ( $M$  is the Misner-Sharp mass [17], defined as  $M = \int_0^R 4\pi\rho r^2 r' dR$ )

$$\dot{E}r' = -2\dot{r}\frac{1+E}{\rho+P}P' = \mp 2\frac{1+E}{\rho+P}P'\alpha\sqrt{2\frac{M}{r} + \frac{1}{3}\Lambda r^2 + E} \quad (4)$$

$$\Rightarrow \dot{E} = 0, E = E(R), \text{ unless there is shell crossing,} \quad (5)$$

$$\dot{M} = -\dot{r}4\pi P r^2 = \mp 4\pi P r^2 \alpha \sqrt{2\frac{M}{r} + \frac{1}{3}\Lambda r^2 + E} = 0 \quad (6)$$

$$\Rightarrow M = M(R), \text{ unless there is shell crossing,} \quad (7)$$

$$\dot{r}^2 = 2\frac{M}{r} + \frac{1}{3}\Lambda r^2 + E. \quad (8)$$

<sup>2</sup>Time derivation of Eq. (8) gives a Raychaudhuri equation related to the gTOV function of Ref. [5]:

$$\text{gTOV} = \frac{M}{r^2} - \frac{\Lambda}{3}r = -\ddot{r}. \quad (9)$$

The dynamical analysis detailed in Ref. [5] yields the motion of separated non-crossing shells in their respective effective potential

$$E = V(r) \equiv -\frac{2M}{r} - \frac{\Lambda}{3}r^2, \quad (10)$$

where the unstable saddle point, for which  $\text{gTOV} = 0$ , gives a local separating shell (see [5], figures 1 and 2, and repeated in Fig. 1), in the case when the shell's energy reaches its critical value. This separating (or "cracking", by analogy with Herrera et al. [18]) shell is characterised by

$$r_{lim} = \sqrt[3]{\frac{3M}{\Lambda}}, \quad (11)$$

$$E_{lim} = -(3M)^{\frac{2}{3}} \Lambda^{\frac{1}{3}} = -\Lambda r_{lim}^2, \quad (12)$$

<sup>1</sup> Actually,  ${}^3R = -2\frac{(Er)'}{r^2}$  so  $E$  is related to the 3-curvature.

<sup>2</sup> In case of shell crossing,  $\dot{E}$  can be nonzero as  $r' = 0$  and  $M$  gets changed by the loss or gain of the mass from infinitesimal shell crossings, so  $E = E(t, R)$  and  $M = M(t, R)$ , in that case.

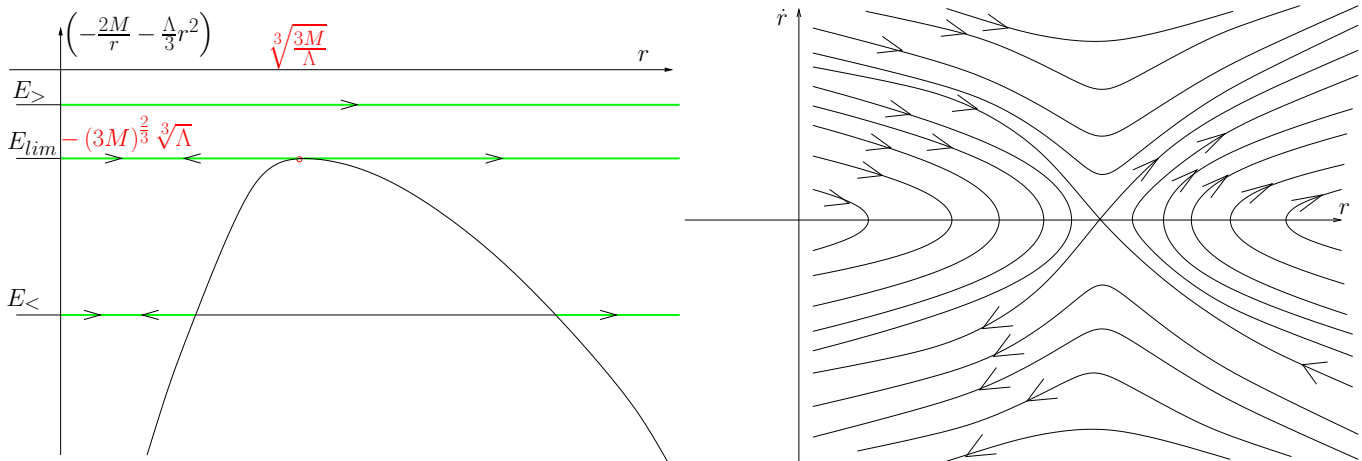


Figure 1. Effective potential kinematic analysis (left) and phase space analysis (right) from [5]. The kinematic analysis for a given shell of constant  $M$  and  $E$  depict the fate of the shell, depending on  $E$  relative to  $E_{lim}$ . It either remains bound ( $E < E_{lim}$ ) or escapes and cosmologically expands ( $E > E_{lim}$ ). There exists a critical behavior where the shell will forever expand, but within a finite, bound radius ( $E = E_{lim}$ ,  $r \leq r_{lim}$ ). The maximum occurs at  $r_{lim} = \sqrt[3]{3M/\Lambda}$ . The corresponding phase space behaviour follows, the scales are set by the value of  $r_{lim} = \sqrt[3]{3M/\Lambda}$  while the actual kinematic of the shell is given by  $E$ .

while the energy follows

$$E = \dot{r}^2 + V(r). \quad (13)$$

**Definition 1.** *Local trapped matter shells in  $\Lambda$ -LTB are defined in GLTB coordinates as the locus  $R_*$  such that*

$$\frac{\Theta}{3} + a \equiv \frac{\dot{r}}{r} = 0 \quad \text{and} \quad \mathcal{L}_n \left( \frac{\Theta}{3} + a \right) \equiv \left( \frac{\dot{r}}{r} \right)' = 0. \quad (14)$$

This definition follows from Eqs. (3.11) and (3.16) of [5] applied to dust with  $\Lambda$ .

In  $\Lambda$ -LTB, conditions (14) are reached by shells at time-infinity which are characterised by Eqs. (8) and (12) so that (see footnote 2)  $E(t = \infty, R_*) = E_{lim}(t = \infty, R_*)$  (defining  $R_*$ ) i.e.<sup>3</sup>

$$\left( \frac{\Theta}{3} + a \right)^2 = 2 \frac{M(R_*)}{r^3(T, R_*)} + \frac{1}{3} \Lambda - \frac{(3M(R_*))^{2/3} \Lambda^{1/3}}{r^2(T, R_*)}. \quad (15)$$

So, since here the Misner-Sharp mass  $M$  and energy  $E$  of each shell is conserved in time (without shell crossing), and  $E$  is thus set by initial  $M(R)$  and  $\dot{r}_i(R)$  profiles, one can characterise local trapped matter, or limit, shell by the intersections  $E = E_{lim}$  (see [5], for details). Global shells emerge from the neighbourhood behaviour around those intersections which local study we give in Secs. III A and III C.

<sup>3</sup> Erratum: Eq. (3.14) of [5] has a sign typo. It should read

$$g_{TOV} = -r \left[ \mathcal{L}_n \left( \frac{\Theta}{3} + a \right) + \left( \frac{\Theta}{3} + a \right)^2 \right].$$

Before studying the occurrence of shell-crossing we will now examine more carefully the role of shear in these settings.

## B. The role of shear in the existence of trapped matter shells

In Ref. [5], we derived the relation between expansion and shear (see Eq. III.10) and found that, in the presently studied model, the shear could be put in the form

$$a = \mp \frac{1}{6 \sqrt{E + 2 \frac{M}{r} + \frac{\Lambda}{3} r^2}} \times \left[ \left( \frac{E'}{r'} - \frac{2E}{r} \right) + \frac{2}{r} \left( \frac{M'}{r'} - \frac{3M}{r} \right) \right]. \quad (16)$$

In the latter equation the terms within the brackets measure the departures from the profiles  $E = \bar{E}(t) r^2$  and  $M = \bar{M}(t) r^3$  that one would expect from a homogeneous, uniformly curved models. Indeed, in FLRW models  $E = k r^2$  and  $M \propto \rho(t) r^3$ . Moreover, we should stress that Eq. (16) yields the shear in terms of non-local (integral) quantities ( $E$  and  $M$ ). We can now evaluate the expansion and shear at the limit shell defined by setting Eqs. (8) and (9) to zero at time infinity in Ref. [5], which, with the conservation of  $E$  and  $M$ , is simply defined by Eqs. (8) and (12). Combining those equations yields

$$E' = - \frac{2M'}{r_{lim}}. \quad (17)$$

First on the limit shell we can write, setting  $E = E_{lim}$ ,

$$a = \mp \frac{\left\{ 2 \frac{M'}{r'} \left( \frac{1}{r} - \frac{1}{r_{lim}} \right) + 2 \Lambda \frac{r_{lim}^2}{r} \left( 1 - \frac{r_{lim}}{r} \right) \right\}}{6 \sqrt{\frac{\Lambda}{3} \left( 2 \frac{r_{lim}^3}{r} + r^2 - 3r_{lim}^2 \right)}}. \quad (18)$$

With the definition of mass issued from Ref. [5]'s Eq. II.27 in GLTB coordinates so

$$M' = 4\pi\rho r^2 r', \quad (19)$$

we then express the shear of the limit shell as

$$a_{lim} = \mp \sqrt{\frac{\Lambda}{3 \left( \frac{r}{r_{lim}} \right)^3} \frac{1 - \frac{4\pi\rho(r)}{\Lambda} \left( \frac{r}{r_{lim}} \right)^3}{\sqrt{2 + \frac{r}{r_{lim}}}}}, \quad (20)$$

which in the limit of time infinity simplifies into

$$a_{lim\infty} = \mp \frac{\Lambda - 4\pi\rho(r_{lim})}{3\sqrt{\Lambda}}. \quad (21)$$

This quantity does not vanish in general. Since at that locus we have  $\Theta = 3 \left( \frac{\dot{r}}{r} - a \right)$ , the expansion then reads

$$\Theta_{lim} = \pm \sqrt{\frac{3\Lambda}{\left( \frac{r}{r_{lim}} \right)^3} \left( \sqrt{2 - 3 \frac{r}{r_{lim}} + \left( \frac{r}{r_{lim}} \right)^3} + \frac{1 - \frac{4\pi\rho(r)}{\Lambda} \left( \frac{r}{r_{lim}} \right)^3}{\sqrt{2 + \frac{r}{r_{lim}}}} \right)}, \quad (22)$$

which in the limit of time infinity simplifies into

$$\Theta_{lim\infty} = \pm \frac{\Lambda - 4\pi\rho(r_{lim})}{\sqrt{\Lambda}}. \quad (23)$$

We shall now use a particular form of initial data in order to study in more detail the role of shear in the appearance of the diving shell. In the examples below we shall assume  $M > 0, \rho > 0, \Lambda > 0$  and  $E < 0$  around the origin.

So, consider analytic initial data for  $\Lambda$ -LTB as in [19, 20]<sup>4</sup>:

$$\begin{aligned} M(R) &= R^3 \sum_{i=0}^{\infty} m_i R^i, \quad m_0 > 0 \\ E(R) &= R^2 \sum_{i=0}^{\infty} E_i R^i, \quad E_0 < 0 \end{aligned} \quad (24)$$

then, from the expressions above, we derive

$$\begin{aligned} a_{lim}(R) &= \pm \Lambda^{1/2} \left( \frac{1}{3} - \frac{2}{3^{2/3}} \left( m_0^{1/3} + \frac{2m_1}{m_0^{2/3}} R + \left( \frac{3m_2}{m_0^{2/3}} - \frac{m_1^2}{m_0^{5/3}} \right) R^2 + O(R^3) \right) \right) \\ r_{lim}(R) &= \left( \frac{3}{\Lambda} \right)^{1/3} \left( m_0^{1/3} R + \frac{m_1}{3m_0^{2/3}} R^2 + O(R^3) \right) \\ E_{lim}(R) &= -3^{2/3} \Lambda^{1/3} \left( m_0^{2/3} R^2 + \frac{2m_1}{3m_0^{1/3}} R^3 + O(R^4) \right) \end{aligned} \quad (25)$$

also, for the re-scaling  $r(t_0, R) = R$ , we get an expression for the initial shear distribution as (see also [21]):

$$\begin{aligned} a(t_0, R) &= \pm \frac{E_1 + 2m_1 R}{6A} \\ &\pm \frac{1}{6} \left( \frac{2E_2 + 4m_2}{A} - \frac{(E_1 + 2m_1)^2}{2A^3} \right) R^2 + O(R^3) \end{aligned}$$

with  $A(R) = \sqrt{E_0 + \Lambda/3 + 2m_0}$ .

It is interesting to see that for a fixed shell  $R$  near the centre, bigger  $M$  (i.e. bigger  $m_3$ ) means smaller initial shear but bigger  $|E_{lim}|$  and  $r_{lim}$  for that shell. On the other hand, since bigger initial shear implies smaller  $|E_{lim}|$  (i.e. smaller departures from  $E_{lim} = 0$ ) and smaller  $r_{lim}$ , one can argue that, at least around the origin (and for the above initial data), shear contributes to the appearance of "cracking" limit shells. This is in agreement with the results of Herrera et al. [18]. We summarize this result as:

**Result 1.** Consider a neighbourhood  $U$  of the origin where the  $\Lambda$ -LTB initial data can be written as (24). Then, bigger values of the initial shear  $|a(t_0, R)|$  in  $U$ , imply smaller  $|E_{lim}|$  and favour the occurrence of trapped matter shells in  $U$ .

For data which is asymptotically Friedmann at infinity we take functions which, at infinity, can be expanded in the form<sup>5</sup>:

$$M(R) = \sum_{i=1}^{+\infty} m_i R^{2/i}, \quad E(R) = \sum_{i=1}^{+\infty} E_i R^{2/i}$$

with  $m_1 \neq 0$  and  $E_1 \neq 0$ . By taking asymptotic expansion

<sup>4</sup> This data ensures that the solution approaches FLRW at the origin which is therefore regular.

<sup>5</sup> Note that we only assume this data form at infinity and not around the origin. Otherwise, we would have a non-regular origin.

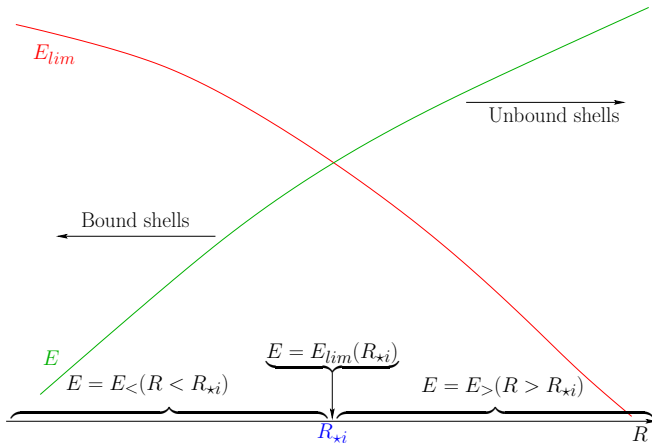


Figure 2. Overcoming local configuration of  $E$  intersecting  $E_{lim}$ . Phase space and effective potential trajectories from dynamical analysis of [5] give the local qualitative behaviour, emphasised on the radial axis. Inner shells on bound trajectories and outer shells on unbound paths forecast no shell crossing locally. Considering  $E_{lim}$  as corresponding to the Newtonian zero radial velocity axis in [24, 25], this configuration is analogous to, e.g., figure 1 of [26].

sions we find :

$$r_{lim}(R) = \left(\frac{3}{\Lambda}\right)^{\frac{1}{3}} \left( m_1^{\frac{1}{3}} R + \frac{m_2}{3m_1^{\frac{2}{3}}} \left(\frac{1}{R}\right)^{\frac{1}{2}} + O\left(\frac{1}{R}\right) \right)$$

$$E_{lim}(R) = -3^{\frac{2}{3}} \Lambda^{\frac{1}{3}} \left( m_1^{\frac{2}{3}} R^2 + \frac{2}{3} \frac{m_2}{m_1^{\frac{1}{3}}} R^{\frac{1}{2}} + \frac{2}{3} \frac{m_3}{m_1^{\frac{1}{3}}} + O\left(\frac{1}{R^{\frac{1}{4}}}\right) \right) \quad (26)$$

while the initial shear is:

$$a(t_0, R) = \mp \frac{E_2}{2\sqrt{3}\sqrt{3E_1 + \Lambda + 6m_1}} \frac{1}{R} + O\left(\frac{1}{R^{\frac{3}{2}}}\right)$$

So, again, bigger values of the initial shear  $|a(t_0, R)|$  near infinity, imply smaller  $|E_{lim}|$  and favour the occurrence of trapped matter shells.

We shall return to this issue in section IV where we study other examples in more detail.

### III. SHELL-CROSSING AND TRAPPED MATTER SHELLS

#### A. Sufficient conditions for shell-crossing

In terms of the comoving coordinates of metric (1), shell-crossing is defined as a surface for which  $\partial_{Rr} = 0$

and the density diverges<sup>6</sup>. In geometrical terms, at shell-crossing there is a discontinuity both in the extrinsic curvature  $K_{ij}$  and in the spacetime metric. For the spacetimes considered here, those discontinuities are finite and the magnitude of the jump in  $K_{ij}$  can be read from the expressions derived in [15, 23].

Hellaby and Lake [6] (see also [7]) have derived necessary and sufficient conditions for the occurrence of shell-crossing in LTB, in terms of the free initial data. Other works have used other type of conditions which are sufficient to avoid shell crossing<sup>7</sup> and therefore imply  $\partial_{Rr} \neq 0$ . For example, in the case of LTB, Landau and Lifshitz [27] simply assume  $\partial_{Rr} > 0$  and, in [28], Hellaby and Lake impose the condition for a simultaneous big bang in their local analysis around the initial singularity.

Here, we shall take a different point of view and write sufficient conditions for the occurrence of shell-crossing in terms of the local behaviour of  $M$  and  $E$  in the neighbourhood of some intersection, when it exists, of the energy  $E$  with the critical energy  $E_{lim}$ . In order to do that we first observe that two local configurations are possible in the neighbourhood of the intersection: either  $E' > E'_{lim}$  or  $E' < E'_{lim}$ .

In the case  $E' > E'_{lim}$ , shells just inside the intersection radius will have a lower  $E$  than their respective  $E_{lim}$  and will therefore be trapped in closed trajectories, following the dynamical analysis presented in Fig. 1. In that case, shells just outside the intersection will display higher  $E$  than their respective  $E_{lim}$  and will accordingly be free to escape to infinity on unbound trajectories. That shell distribution will lead to the separation of neighbouring shells, those inside the intersection being bound to a finite region while those outside will escape to infinity. This case doesn't entail neighbouring shell crossings and is presented on Fig. 2.

On the contrary, in the case  $E' < E'_{lim}$ , shells just inside the intersection will have a higher  $E$  than their respective  $E_{lim}$  and will accordingly be free to escape to infinity on unbound trajectories whereas shells just outside the intersection will display a lower  $E$  than their respective  $E_{lim}$  and will therefore be trapped in closed trajectories. Because of the configuration of that shell distribution, shell crossings of neighbouring shells occur: those inside the intersection escaping to infinity will have to cross those outside which are bound to a finite region. This case is presented on Fig. 3. We summarize this result as:

**Result 2.** *Let  $\Delta = E - E_{lim}$  and consider a  $\Lambda$ -LTB spacetime where there is  $R_*$  such that  $\Delta|_{R_*} = 0$ . Then,*

<sup>6</sup> There can exist cases where  $\partial_{Rr} = 0$  and the density does not diverge. At those regular extrema, the extrinsic curvature is discontinuous while the metric is continuous and finite [6, 22].

<sup>7</sup> A comment on the occurrence of caustics when using a synchronous reference frame can be found in Ref. [27] (§97). We must notice though that the latter assumes that the strong energy condition holds, whereas in our present case the cosmological constant evades that assumption.



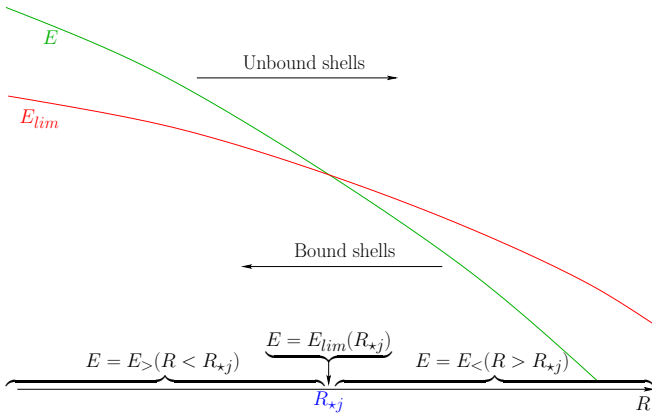


Figure 3. Undercoming local configuration of  $E$  intersecting  $E_{lim}$ . Phase space and effective potential trajectories from dynamical analysis of [5] give the local qualitative behaviour, emphasised on the radial axis. Outer shells on bound trajectories and inner shells on unbound paths will lead to local shell crossing. Considering  $E_{lim}$  as corresponding to the Newtonian zero radial velocity axis in [24, 25], this configuration is similar to, e.g., figure 2b of [24].

a sufficient condition for the existence of shell crossing is  $\Delta'|_{R_*} < 0$ .

We point out that, for  $\Lambda = 0$ , our condition leads to  $E' < 0$ , which is the condition implicitly considered in [6, 7]<sup>8</sup>. In that case, we simply obtain  $E'_{lim} = -8\pi\rho r^2 r' \left(\frac{\Lambda}{3M}\right)^{\frac{1}{3}} = 0$ . In this sense, our sufficient condition generalises, for  $\Lambda \neq 0$ , the result of Ref. [6, 7]<sup>9</sup>. We also note that their condition on bang times  $t'_b(R)$  is  $t'_b(R) \leq 0$ , while we can also allow for  $t'_b(R) > 0$  as long as  $t_b(R)$  is less than the initial time  $t_0$  considered here.

There is an interesting analogy between our shell-crossing condition and a similar condition in Newtonian theory. In fact, the Newtonian approach used in [24, 25] considers kinematic configurations in velocity-radius two dimensional phase space which lead to one (and three) dimensional Zel'Dovich pancakes (see Refs. [25, 29, 30] for the classical cosmological spherical context). Their behaviour is similar to the local evolutions of the dynamical configurations in Figs. 2 and 3. While in [24, 25] the

<sup>8</sup> For LTB with  $\Lambda = 0$ , we recall that the necessary and sufficient conditions for no-shell crossing in [6] are:

$$T'_B \leq 0, E' \geq 0, M' \geq 0$$

where  $T_B$  is the bang time, while the necessary and sufficient conditions for no-shell crossing in [7] are:

$$T'_B \leq 0, E' > 0, M' \geq 0.$$

Therefore, if one of these conditions fails then there will be shell crossing.

<sup>9</sup> Although our interest is in the neighbourhood of radius where  $\Delta = 0$ , our analysis can be extended to other locations.

authors take the radial axis to separate collapsing and expanding kinematics, here we take  $E_{lim}$  locally as a deformed radial axis.

## B. Hypotheses and dynamical analysis

Since part of our analysis is based on the  $E - E_{lim}$  diagram, it is useful to clarify the constraints introduced by the set of hypotheses we propose.

### 1. Regular density distribution

A regular density distribution is motivated by standard cosmological models [11, 29, e.g.]. In the weak energy condition, the density remains positive so the mass profile is initially always monotonously increasing, thus  $E_{lim}$ , from Eq. 12, is initially always monotonously decreasing,

$$\frac{\partial M}{\partial R} \geq 0 \Rightarrow \frac{\partial E_{lim}}{\partial R} \leq 0. \quad (27)$$

The regularity implies finiteness of the mass and nonzero values for the density at the centre. This constraints their logarithmic slope in the following manner: suppose a value  $-\epsilon$  for the slope of the density in the centre ( $\rho \propto r^{-\epsilon}$ ), then the mass shall behave accordingly as  $r^{3-\epsilon}$ . Finiteness of the mass implies then  $\epsilon \leq 3$  and no vacuum in the centre implies  $\epsilon \geq 0$ , from the density.

### 2. Initial Hubble-type flow

This simplifies the initial velocity profile into one that only admits outgoing radial velocities (positive  $\dot{r}$ ), in the fashion of expanding initial conditions in a Hubble flow, although less restrictive. As a consequence of this and the previous condition, the profiles in the centre always respect, in initial conditions, the hierarchy  $E < E_{lim}$ , which is crucial for the emergence of a bound core. In this case

$$E_{lim} = -(3M)^{\frac{2}{3}} \Lambda^{\frac{1}{3}} \sim R^{2-\frac{2}{3}\epsilon} \rightarrow 0 \text{ as } \epsilon \leq 3, \\ R \rightarrow 0 \\ E = \dot{r}^2 - \frac{2M}{R} - \frac{\Lambda}{3} R^2 \sim -R^{2-\epsilon} \rightarrow 0, \\ R \rightarrow 0$$

since  $\dot{r} \sim R \rightarrow 0$  so the  $\dot{r}^2$  and  $\frac{\Lambda}{3} R^2$  both tend to zero as  $R \rightarrow 0$

zero as  $R^2$  and are thus dominated by the  $-\frac{2M}{R}$  term for  $\epsilon > 0$ . Thus around the centre,

$$\frac{E}{E_{lim}} \underset{R \rightarrow 0}{\sim} = \frac{2}{3^{\frac{2}{3}} R} \left(\frac{M}{\Lambda}\right)^{\frac{1}{3}} \\ \underset{R \rightarrow 0}{\sim} \frac{2}{3^{\frac{2}{3}} \Lambda^{\frac{1}{3}}} R^{-\frac{\epsilon}{3}} > 1$$

$$\Rightarrow E < E_{lim}, \text{ for } \epsilon > 0, E_{lim} < 0.$$

In the peculiar case of a constant central density ( $\epsilon = 0$ ), we have  $M \sim \frac{4\pi}{3}\rho_0 R^3$ ,  $\dot{r} \sim \partial_R \dot{r}_0 R = H_c R$  so  $R \rightarrow 0$   $R \rightarrow 0$   
 $E = (H_c^2 - \frac{8\pi}{3}\rho_0 - \frac{\Lambda}{3}) R^2 = (H_c^2 - \frac{8\pi}{3}(\rho_0 + \rho_\Lambda)) R^2$ . In that case, the Hubble-type flow needs to remain moderate in the centre to respect the constraint

$$\partial_R \dot{r}_0 < 4\pi \left( \rho_0^{\frac{2}{3}} (2\rho_\Lambda)^{\frac{1}{3}} + \frac{2}{3}(\rho_0 + \rho_\Lambda) \right).$$

In the rest of the paper, we assume the conditions for  $E < E_{lim}$  in the centre are met.

### 3. Asymptotic spatial cosmological behaviour

If we restrict our explorations to *asymptotically cosmological* (FLRW) solutions, this implies that at radial infinity the mass and velocity initial profiles, constraining the energy and  $E_{lim}$  profiles for all time, shall obey

$$\begin{aligned} M &\xrightarrow{R \rightarrow \infty} \frac{4\pi}{3}\rho_b R^3 \text{ with } \frac{3M}{4\pi R^3} \xrightarrow{R \rightarrow \infty} \rho_b = \rho_b(t) \\ &\Rightarrow E_{lim} \xrightarrow{R \rightarrow \infty} - (4\pi\rho_b)^{\frac{2}{3}} \Lambda^{\frac{1}{3}} R^2, \\ \dot{r}_i(R) &\xrightarrow{R \rightarrow \infty} H_i R \Rightarrow E \xrightarrow{R \rightarrow \infty} -K R^2. \end{aligned} \quad (28)$$

We note that the value of the curvature  $K$  of the asymptotic FLRW solution compared with the equivalent  $(4\pi\rho_b)^{\frac{2}{3}} \Lambda^{\frac{1}{3}}$  FLRW critical curvature will determine, together with the central constraint  $E < E_{lim}$ , the occurrence of, at least, one intersection of  $E$  and  $E_{lim}$  of the  $E' > E'_{lim}$  kind, not inductive of shell crossing (see Sec. III A).

**Definition 2.** *Supposing there exists  $n \in \mathbb{N}$  shells verifying equation (15), we order them by initial radius and denote them  $R_{*i}$ ,  $i \in [1, n]$ ,*

- $R_{*out} \equiv R_{*n}$  the outermost intersections  $E = E_{lim}$  of the initial profiles
- $R_{*in} \equiv R_{*1}$  the innermost initial intersections  $E = E_{lim}$  of the initial profiles.

### 4. Local mass conservation and Lagrangian frame

Since in our system, the cosmological constant is inert by definition and dust purely interacts gravitationally, we assume, as in [15], that *the rest mass of each crossing infinitesimal shell is conserved*. The shell crossing event can thus be viewed as an infinitesimal exchange of the relative positions and integrated masses while each shell conserves its own velocity.

As shell masses  $M$  and energies  $E$  are conserved between shell crossing events, Eq. (8) will govern the motion of individual shells. Keeping initial  $R = r(0, R)$

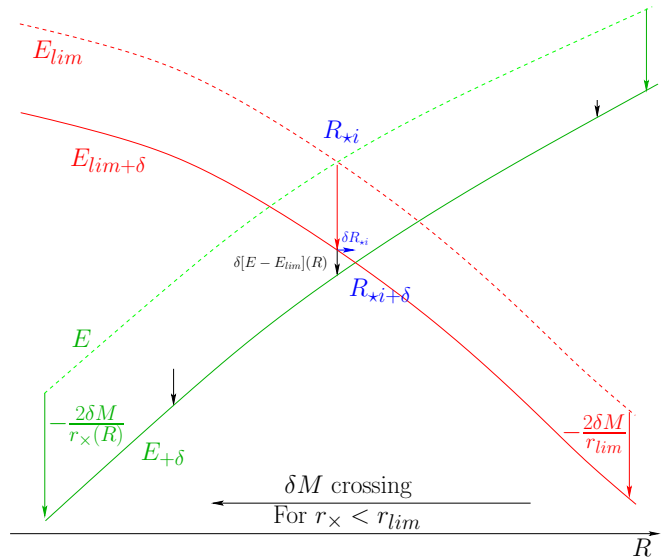


Figure 4. Effect of an ingoing, infinitesimal test shell-crossing on the energy and critical energy profiles, around the *local* initial configuration for the overcoming of  $E_{lim}$  by  $E$ . The initial intersection shell becomes bound on such perturbations and the local intersection shell shifts outwards in radius.

as Lagrangian labels, we can follow the dynamics of the shells using a the simple prescription obtained above without the need to reorder the radial labels as would require a metric extension. Instead, we keep the initial labels all throughout and follow each shell's evolution using Eq. (8) and the shell crossing prescription of Sec. III B 4, as e.g. in Ref [24, 29].

### C. Local effects of shell crossing on trapped matter shells

In this section, we will detail how a test crossing shell affects locally the values of  $E$  and  $E_{lim}$  around trapped matter shells.

Since each shell conserves its infinitesimal mass, the local effect of an elementary crossing of a system's shell by a test, neighbouring, shell will just exchange their non-local mass in the exchange of their positions<sup>10</sup>. As a consequence, their values of  $E$  and  $E_{lim}$  will also change. The change of  $E$ , in Eq. (4), is allowed by the shell crossing event.

A shell crossed at some  $r_x$  by an infinitesimal mass  $\delta M$  ( $\delta M > 0$  for inward crossing,  $< 0$  for outward crossing) will see its values shifted as follow (the reciprocal is true

<sup>10</sup> In this process the other shells of the system, not involved, will remain unaffected and conserve their masses.

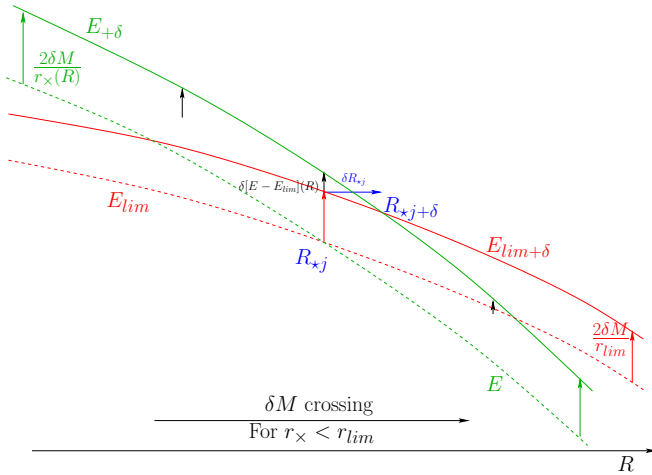


Figure 5. Effect of an outgoing, infinitesimal shell-crossing on the energy and critical energy profiles, around the *local* initial configuration for the undercoming of  $E_{lim}$  by  $E$ . The initial intersection shell becomes unbound on such perturbations and the local intersection shell shifts outwards in radius.

for the crossing shell with  $-\delta M$ )

$$E_{+\delta} = E - \frac{2\delta M}{r_{\times}}, \quad (29)$$

$$E_{lim+\delta} \simeq E_{lim} + \frac{2}{3} \frac{\delta M}{M} E_{lim}. \quad (30)$$

Thus, for an inward (resp. outward) crossing, both  $E$  and  $E_{lim}$  will decrease (resp. increase). Their relative separation, crucial around intersections, will follow

$$\delta\Delta \simeq 2\delta M \left( \frac{1}{r_{lim}} - \frac{1}{r_{\times}} \right), \quad (31)$$

which generalises the conditions from [6, 7] (see Result 2). The sign of this shift is determined by the initial position  $r(t_0, R) = R = r_i$  of shells with respect to their  $r_{lim}$ .

Bound shells can never cross their respective  $r_{lim}$  and shells with  $E = E_{lim}$  reach their  $r_{lim}$  at infinity in time. Thus crossing events involving one bound shell, satisfy  $\left( \frac{1}{r_{lim}} - \frac{1}{r_{\times}} \right) < 0$ . However, once escaping shells go beyond their respective  $r_{lim}$ , they experience the opposite relative effect on their  $\delta\Delta$ . Thus, it is possible to have a crossing of two escaping shells beyond their respective  $r_{lim}$  that produce shifts in the opposite direction. However, once beyond their  $r_{lim}$ , even drastic changes cannot put shells on closed orbits linked with the centre as they would correspond to points on the outer side of the effective potential (Fig. 1a). Since intersections  $E = E_{lim}$  take place in the neighbourhood of bound shells (those with  $E$  under their  $E_{lim}$ ) we can restrict ourselves to consider local shell crossing in  $r_{\times} < r_{lim}$ .

To first order, for inward-going crossing shells, we have  $\delta\Delta < 0$ , as illustrated on Figs. 4 and 7, while outward-going shells have  $\delta\Delta > 0$ , see Figs. 6 and 5. As a

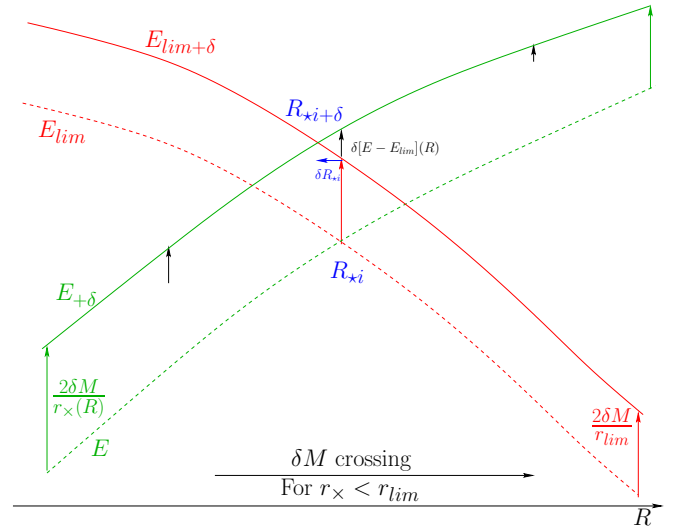


Figure 6. Effect of an outgoing, infinitesimal shell-crossing on the energy and critical energy profiles, around the *local* initial configuration for the overcoming of  $E_{lim}$  by  $E$ . The initial intersection shell becomes unbound on such perturbations and the local intersection shell shifts inwards in radius.

consequence, the limit shell defined by the intersection shifts forward (resp. backward) for the two cases of local configurations. The resulting cases are overcoming inward crossings and undercoming outward crossings (resp. overcoming outward crossings and undercoming inward crossings) and are illustrated on Figs. 4 and 5 (resp. 6 and 7).

To simplify the qualitative study of the system, we will first consider a prescription where both  $M$  and  $E$  are conserved, in Secs. III D 1 and III D 2. We will then drop this assumption and include the evolution of trapped matter shells' neighbourhoods, building from infinitesimal shell crossing as described below in Sec. III D 3 to ascertain the qualitative evolution of the system, in Sec. III D 4.

#### D. Global effect of shell crossing on limit trapped matter shells

##### 1. Simplest model with shell crossing

In order to study the simplest set of initial conditions where shell crossing occurs, given the constraints of sec. III B from Result 2, we shall consider a model with a single undercoming configuration. The topological constraints coming from the two dimensional  $E$  vs.  $R$  diagrams<sup>11</sup>, together with the choice of an open background

<sup>11</sup> For example in the centre ( $E < E_{lim}$ ). See Fig. 8.



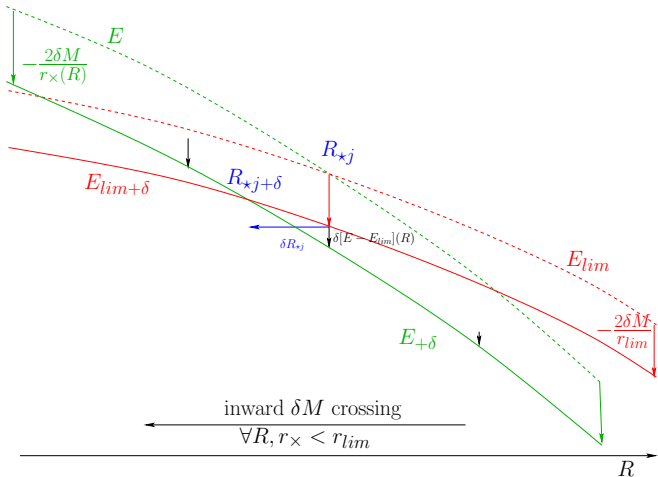


Figure 7. Effect of an ingoing, infinitesimal test shell-crossing on the energy and critical energy profiles, around the *local* initial configuration for the undercoming of  $E_{lim}$  by  $E$ . The initial intersection shell becomes bound on such perturbations and the intersection shell shifts inwards in radius.

at infinity<sup>12</sup> leads to initial conditions for  $E$  and  $E_{lim}$  with three intersections (see Fig. 8), the middle one verifying Result 2. We thus have a model with  $R_{*1} = R_{*in}$ ,  $R_{*2}$  and  $R_{*3} = R_{*out}$  defined in its initial conditions. We can now consider the *inner system*, also called the *system*, to be circumscribed by  $R_{*out}$ . Unbound shells inside this system are in position to escape it and hence define a remarkable shell outside the system:

**Remark 1.** *The inner or non-bound shells of initial conditions in  $E$  and  $E_{lim}$  induce a few remarkable features defined as follows:*

- We will consider all shells inside  $R_{*out}$  as the initial inner system.
- We will denote by  $E_{max}$  the maximum value of non-bound  $E$  in the set of shells inside  $R_{*out}$  or outside of it but with horizontal tangent, i.e.  $E_{max} = \max\{E : ((E' = 0) \vee (0 < R \leq R_{*out})) \wedge (E \geq E_{lim})\}$
- $R_{max}$  is the largest value for which  $E = E_{max}$ , i.e.  $R_{max} = \max\{R : E(R) = E_{max}\}$
- $R_{free}$  is the furthest shell outside  $R_{*out}$  with increasing  $E = E_{max}$ , when it exists, i.e.  $R_{free} = \max\{R : (R \geq R_{*out}) \wedge (E = E_{max}) \wedge (E'(R) > 0)\}$
- We will note  $E_{free}$  the value of  $E$ , when it exists, as  $E_{free} = E(t = t_0, R_{free})$ .

With the above definitions, we will now examine the effects of shell crossing on trapped matter shells.

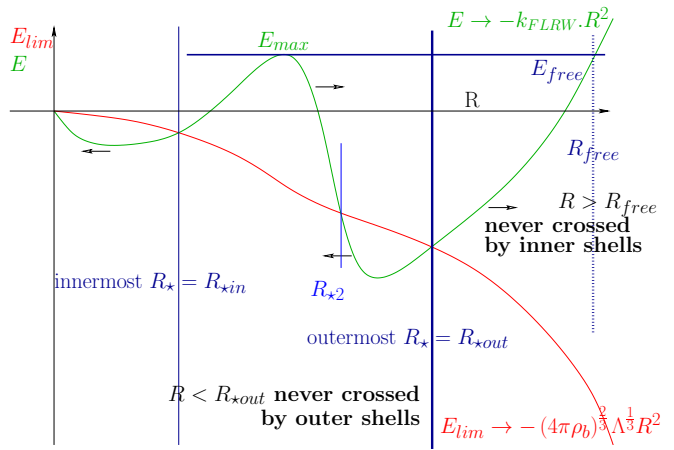


Figure 8. Open background with arbitrary central mass distribution and a single local undercoming intersection. It always gives protected inner shells as well as unmodified cosmological expansion, when keeping integrability despite shell-crossing. Shell crossing entails no fundamental modification.

## 2. Limit trapped matter shells in the integrable dynamical system

In a model where both  $M$  and  $E$  are conserved through shell crossings, we can extend the analysis of [5], as each shell's dynamics remains integrable and is governed by the Lagrangian Eq. (8)<sup>13</sup>. In this case, the qualitative dynamical behaviour of the system is entirely determined from the shape of its initial conditions in a  $E$  and  $E_{lim}$  vs.  $R$  diagram.

As we will see in Sec. IIID 4, when including the full effects of shell crossing on  $E$  and  $E_{lim}$ , the key properties of trapped matter shells will be obtained in the limit  $t \rightarrow \infty$ . Since in this section,  $M$  and  $E$  are assumed to be conserved with time, all the properties deduced here will remain unchanged in that limit. We will therefore express our results in the limit  $t \rightarrow \infty$ , using definitions which evolve from Rem. 1 and are detailed in Appendix A.

From Fig. 8, we can see that all the bound shells will remain under  $r_{lim*out} = r_{lim}(R_{*out})$ , while all unbound shell of the inner system will escape it<sup>14</sup>. Thus, considering that bound shells will eventually turnaround and orbit back and forth between the centre and their turnaround radius, we find that all shells inside  $r(t, R) = r_{lim*out}$  will be crossed from both sides (interior and exterior)<sup>15</sup>. Only the shell  $R_{*out}$  will remain uncrossed from outside shells. This leads to the following definition:

<sup>12</sup> This means  $E \rightarrow -k_{FLRW} \cdot R^2$  with  $k_{FLRW} < 0$  and  $R \rightarrow \infty$

$$E_{lim} \rightarrow -(4\pi\rho_b)^{\frac{2}{3}} \Lambda^{\frac{1}{3}} \cdot R^2$$

<sup>13</sup> The final fate of each shell will always remain on horizontal lines and their gravitational nature, whether bound or unbound will also remain the same throughout their history.

<sup>14</sup> This is indicated on Fig. 8 by horizontal arrows.

<sup>15</sup> This includes the  $R_{*in}$  and  $R_{*2}$  shells, locally considered trapped matter shells.

**Definition 3.** *The outer limit trapped matter shell  $R_{t^*\text{out}\infty}$  verifies Def. 1 in the limit  $t \rightarrow \infty$ , in addition to being the outermost such shell which locally is not shell-crossing inductive<sup>16</sup> i.e.*

$$R_{t^*\text{out}\infty} = \{R : \max\{R_{*\infty}\} \wedge (E'(t \rightarrow \infty) > E'_{lim}(t \rightarrow \infty))\}$$

Note, from Def. 2, that  $R_{*\text{out}}$ : verifies Def. 3; defines  $R_{t^*\text{out}}$ , if  $E' > E'_{lim}$ ; and verifies  $R_{t^*\text{out}} = R_{t^*\text{out}\infty}$  in the limit  $t \rightarrow \infty$ .

**Remark 2.** *In  $\Lambda$ -LTB with asymptotic cosmological evolution (FLRW at radial infinity) and initial Hubble-like flow (outwards going) for which shell crossing occurs, the outer limit trapped matter shell is a surface  $S$  with the following properties:*

- *The matter exterior to  $S$  follows trapped geodesics, remaining in that exterior.*
- *The matter inside  $S$  can expand and collapse protected from the crossing of outside shells.*
- *$S$  is the shell with largest  $R$  for which the energy  $E$  intersects the critical energy  $E_{lim}$ , from bound to unbound shells.*

The condition for existence of  $R_{t^*\text{out}\infty}$ , follows from the properties of  $R_{t^*\text{out}}$ , so we obtain the following result:

**Result 3.** *Sufficient conditions for the existence of an outer limit trapped matter shell are:*

- *The FLRW curvature of the background  $k_{FLRW} < (4\pi\rho_b)^{\frac{2}{3}} \Lambda^{\frac{1}{3}}$ , or*
- *$R_{t^*\text{out}}$  exists, or*
- *The local configuration around  $R_{*\text{out}}$  is such that  $E'_{*\text{out}} > E'_{lim*\text{out}}$ .*

*Proof.*  $k_{FLRW} < (4\pi\rho_b)^{\frac{2}{3}} \Lambda^{\frac{1}{3}} \Rightarrow E(R \rightarrow \infty) > E_{lim}(R \rightarrow \infty)$  so the last intersection  $E(R) = E_{lim}(R)$  is such that  $E' > E'_{lim}$  from a corollary to Bolzano-Weierstrass theorem and the Definition 3 is verified.  $\square$

We show, in Fig. 8, a diagram with data such that the inner limit trapped matter shell  $R_{t^*\text{out}}$  is at  $R_{*\text{out}}$ . The exterior of the system will include all the unbound shells escaping to infinity. However, the dynamics from Eq. (8) allows us to study under what conditions unbound system's shells will never cross shells located in the exterior of the system<sup>17</sup>. Take two different shells  $R_1 < R_2$ , eventually crossing each other at a given radius<sup>18</sup>  $r_\times$ , and with the outer shell more open than the inner shell (i.e.

$E_1 < E_2$  for  $M_1 < M_2$ ):

$$E_1 = v_1^2 - \frac{\Lambda}{3} r_\times^2 - \frac{2M_1}{r_\times}, \text{ with } E_1 < E_2, \quad (32)$$

$$E_2 = v_2^2 - \frac{\Lambda}{3} r_\times^2 - \frac{2M_2}{r_\times} \text{ and } M_1 < M_2, \quad (33)$$

$$\Rightarrow \Delta v^2 = \Delta E + \frac{2\Delta M}{r_\times} > 0 \text{ and } \quad (34)$$

$$\Delta v^2 \underset{r_\times \rightarrow \infty}{\sim} \Delta E > 0 \Rightarrow \forall t, v_2^2 > v_1^2. \quad (35)$$

Thence shells with  $E_1 < E_2$  and  $M_1 < M_2$  will always remain in the same radial order and the shell with  $E = E_{max}$  will then escape all other system's shells. It then appears that, when  $R_{free}$  exists, all shells with  $E > E_{free}$  will never be crossed by any shell inside  $R_{free}$ . The counterpart to Def. 3 can thus be formulated by defining first  $E_{max}$ . In turn, the condition for the existence of  $E_{max}$  is that  $E \geq E_{lim}$ , in the limit  $t \rightarrow \infty$ . Thus, Rem. 1 can be adapted here as<sup>19</sup>

**Definition 4.** *Suppose  $E_{max\infty}$  exists and is defined, in the initial conditions, as*

$$E_{max\infty} = \max \left\{ E|_{(t \rightarrow \infty)} : ((E' = 0) \vee (0 < R \leq R_{*\text{out}\infty})) \wedge (E \geq E_{lim})_{(t \rightarrow \infty)} \right\}. \quad (36)$$

*Then, inner limit trapped matter shells are defined as the locus  $R_{free\infty}$  such that*

$$R_{free\infty} = \max \{ R : (R \geq R_{*\text{out}\infty}) \wedge (E = E_{max\infty})_{t \rightarrow \infty} \wedge (E'(t \rightarrow \infty, R) > 0) \}. \quad (37)$$

**Remark 3.** *In  $\Lambda$ -LTB with asymptotic cosmological evolution (FLRW at radial infinity) and initial Hubble-like flow (outwards going) for which shell crossing occurs (and  $E_{max\infty}$  is defined), the inner limit trapped matter shell is a surface  $S$  with the following properties:*

- *The matter interior to  $S$  follows trapped geodesics which remain in that interior.*
- *The matter exterior to  $S$  expands, protected from the crossing of inside shells.*
- *$S$  is the shell outside the system (defined with  $R_{*\text{out}\infty}$ ) with energy equal to that of the highest  $E$  of non-bound shells, and starting inside of the system, or outside it but with horizontal tangent.*

The conditions for existence of  $R_{free\infty}$  combine the existence of  $E_{max\infty}$  with constraints on the background:

<sup>16</sup> Recall that  $R_{*\infty}$  is defined by solutions in initial  $R$  of Eq. 15 taken at  $t \rightarrow \infty$ .

<sup>17</sup> Their escape velocity at infinity should never exceed that of exterior shells.

<sup>18</sup> This radius is allowed to tend to radial infinity.

<sup>19</sup> The following can be formulated also in terms of gauge invariant Lie derivatives, expansion and shear, as seen in appendix B.

**Result 4.** *Sufficient conditions for the existence of an inner limit trapped matter shell are (a) the existence of  $E_{max\infty}$  and (b) the existence of  $E_{free\infty}$ :*

- (a) • *There exist initially a non-bound, system shell, or a non-bound shell with horizontal tangent:  $\exists R : (0 < R \leq R_{\star out} \vee E' = 0) \wedge E(R) \geq E_{lim}(R)$ , or*
- $R_{\star out\infty}$  exists, or
  - *There exist at least one  $R_{\star i}$*
- (b) •  $E_{max\infty} < E(R \rightarrow \infty)$ , or
- $\exists R : R \geq R_{\star out\infty} \wedge E(t \rightarrow \infty, R) = E_{max\infty} \wedge E'(R) > 0$

*Proof.* (a) 1/ If we have  $R$  such that  $(0 < R \leq R_{\star out} \vee E' = 0) \wedge E(R) > E_{lim}(R)$ , then, either it is a maximum so  $E_{max}$  exists and, by time evolution of its neighbourhood,  $E_{max\infty}$  exists, or, by continuity, in the case when it is not a shell with  $E' = 0$  (local maximum), there is a shell with larger  $E$  which satisfies Rem. 1 for  $E_{max}$  and thus one in its neighbourhood satisfying Def. 5 for  $E_{max\infty}$ .

2/ If  $R_{\star out\infty}$  exists, it is not bound at time infinity and is inside the system, therefore, even if it is the only unbound system shell, it can at least define  $E_{max\infty}$ .

3/ If there is only one  $R_{\star}$ , then it is  $R_{\star out}$  by Def. 2. We are then in the case 2/ above as this guarantees the existence of  $R_{\star out\infty}$ .

(b) Since: (i)  $E_{max\infty}$  is, by definition, the largest value of  $E$  reached at time infinity by inner or outer local maxima shells,

(ii) uncrossed outer shells have their  $E$  conserved,

(iii) asymptotic cosmological conditions render  $E$  monotonous near infinity,

(iv) evolution of the inner shell  $R_{max\infty}$  follows Eqs. 35,

(v) the energy profile is continuous,

therefore,  $E_{\star out\infty} \leq E_{max\infty}$  and by continuity, since  $E_{max\infty} < E(R \rightarrow \infty)$ , exterior shells will obey  $E \in [E_{\star out\infty}, E(t \rightarrow \infty, R \rightarrow \infty)] \supseteq [E_{max\infty}, E(t \rightarrow \infty, R \rightarrow \infty)]$ , thus there exist at least one shell at time infinity with  $E = E_{max\infty}$ .

Moreover, for the outermost exterior shell  $R_{xmax\infty} = \max\{R : R \geq R_{\star out\infty}, E(R) = E_{max\infty}\}$  with  $E = E_{max\infty}$ , since  $E_{max\infty} < E(R \rightarrow \infty)$ , by continuity, all shells outside of it will verify  $E > E_{max\infty}$ . Therefore  $E'(R_{xmax\infty}) > 0$  and  $R_{xmax\infty} = R_{free\infty}$  is fulfilling Def. 4.  $\square$

We show a diagram in Fig. 8 where we indicate the outer limit trapped matter shell for which  $R_{free} = R_{free\infty}$ , in the model where both  $E$  and  $M$  are conserved between shell crossings. We thus have found, for that model, that extending the analysis of [5] in the context of shell crossing leads to the emergence of two remarkable shells: an inner limit trapped matter shell and an outer limit trapped matter shell. From their definitions 3 and 4, we can deduce other properties depending on the background cosmological model, namely:

From Result 3, any background with  $E > E_{lim}$  will admit an outer limit trapped matter shell. This includes some closed models and all flat and open models.

From Result 4, and under the assumptions of this section, any closed background in our models cannot foster an inner limit trapped matter shell as the finite value of  $E_{max\infty}$  is always larger than its energy at radial infinity. Conversely, open models always have an inner limit trapped matter shell (see the example of section IV) and only flat models with moderate enough energy fluctuations (i.e. for which  $E_{max} < 0 = E(R \rightarrow \infty)$ ) can allow the existence of an inner limit trapped matter shell. In summary:

**Summary 1.** *Consider a  $\Lambda$ -LTB spacetime with asymptotic cosmological evolution (FLRW at radial infinity) and initial Hubble-like flow (outwards going) for which shell crossing occurs. Then:*

1. *The global limit trapped matter shell found in the no-shell crossing  $\Lambda$ -LTB examples of [5] is split, if shell crossing occurs, into at most, two global shells, namely an inner limit trapped matter shell and an outer limit trapped matter shell.*
2. *For open or flat expanding spacetimes,*
  - (a) *there exists always an outer limit trapped matter shell at  $R_{t\star out\infty}$ .*
  - (b) *The inner limit trapped matter shell exists in flat backgrounds for sufficiently small initial velocities inside the system limited by  $R_{\star out\infty}$ .*
3. *For closed spacetimes, outer limit trapped matter shells are present if  $k_{FLRW} < (4\pi\rho_b)^{\frac{2}{3}} \Lambda^{\frac{1}{3}}$  and inner limit trapped matter shells cannot be defined if shell crossing occurs, with our definitions.*
4. *In the  $\Lambda$ -CDM examples of global limit trapped matter shell found in [5], inner and outer limit trapped matter shells reduce to one single surface.*

*Proof.* 1: Direct from Definitions 3 and 4 and Result 2 which leads to shell crossings at some  $R_{\star}$ .

2(a): From Result 3.

2(b): Direct from Result 4, as open and flat expanding spacetimes admit  $E(R \rightarrow \infty) \geq 0$ . Some flat spacetimes can exhibit  $E_{free\infty} > 0$  while their  $E \rightarrow 0$ . For  $R \rightarrow \infty$

those cases, Definition 4 is never verified.

3: Using Result 3, for closed spacetimes,  $E \rightarrow -$   
 $R \rightarrow \infty$

$\infty \ll E_{free\infty}$ , so from Result 4, Definition 4 is never verified.

4: Applying Definitions 3 and 4 to configurations where there is only one intersection  $R_{\star} = R_{\star 1} = R_{\star out}$  verifying  $E' > E'_{lim}$ , no shell crossing occurs. Thus all  $E$  values are constant over time so  $R_{\star out} = R_{t\star out\infty}$ , and given the open background,  $E_{free} = E_{\star out}$ , so  $R_{free\infty} = R_{\star out} = R_{t\star out\infty}$ .  $\square$

In this section, we have assumed that  $E$  and  $M$  were conserved through shell crossings. In the next section, we drop this assumption and investigate whether our previous results remain true.

### 3. Global effect of shell crossing

Since the sign of  $\Delta = E - E_{lim}$  determines the binding property of the system, it is useful to give the final values of  $E$  and  $E_{lim}$  for each shell, labeled  $i$ , in terms of the initial  $R_i$  and  $M_i$ , reaching areal radius  $r$  after crossing shells, with

$$M(r(R, t), t) = M_i + \int dM_{in} - \int dM_{out} = M_i + \Delta M_i$$

where the index *in* refers to inward crossing, *out* to outward crossing,  $j$  to the shells crossing shell  $i$ .

Using definition (12) and integrating Eq. (29) over all crossing shells, we get

$$E_{lim}(r) = E_{lim}(R_i) - \left[ \left( 1 + \frac{\Delta M_i}{M_i} \right)^{\frac{2}{3}} - 1 \right] \frac{3M_i}{r_{lim}(R_i)}, \quad (38)$$

$$E(r) = E(R_i) - 8\pi \left[ \int dr_{j,in} - \int dr_{j,out} \right] \frac{\rho(r_j) r_j^2}{r_{\times i}(r_j)}, \quad (39)$$

where  $r_{\times i}$  is a crossing radius. Because of their qualitatively simple shell crossing histories, we can look at the changes for three peculiar shells, singled out on Fig. 8: the innermost limit shell, the outermost limit shell and the maximum  $E$  shell initially lying in the interior of the outermost limit shell.

The innermost limit shell will only be crossed by more bound shells exterior to it, so  $\Delta M_1 > 0$  and

$$E(r(R_{\star 1})) = E(R_{\star 1}) - 8\pi \int dr_{j,in} \frac{\rho(r_j) r_j^2}{r_{\times 1}(r_j)}. \quad (40)$$

Since

$$\frac{1}{3} \left( \frac{\Delta M_1}{M_1} \right)^2 + \left( \frac{2}{3} \frac{\Delta M_1}{M_1} \right)^3 > 0 \quad (41)$$

$$\Leftrightarrow \left[ \left( 1 + \frac{\Delta M_1}{M_1} \right)^{\frac{2}{3}} - 1 \right] < \frac{2}{3} \frac{\Delta M_1}{M_1} \quad (42)$$

and

$$-\frac{1}{r_{\times 1}(r_j)} < -\frac{1}{\max[r_{\times 1}(r_j)]} < -\frac{1}{r_{lim}(R_{\star 1})}, \quad (43)$$

as the innermost limit shell becomes a bound shell, we get that

$$\Delta [E - E_{lim}]_1 < 2\Delta M_1 \left[ \frac{1}{r_{lim}(R_{\star 1})} - \frac{1}{\max[r_{\times 1}(r_j)]} \right] < 0. \quad (44)$$

Thus, the innermost limit shell will globally shift outwards, following the qualitative analysis of Fig. 4.

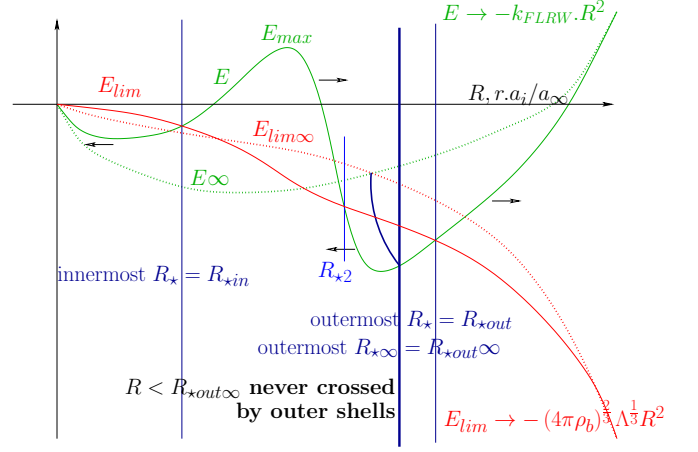


Figure 9. Illustration, on an open background with arbitrary central mass distribution, of the effect of shell crossing on the inner global limit shell previously defined as the outermost local limit shell. The time variation of the locus of the outermost local limit shell leads to defining it as the time infinity outermost limit shell: this is shown on the extrapolated time infinity energy profiles and linked to the initial energy profile by a connecting curve. The global inner limit shell is then just shifted inwards, compared with the integrable analysis.

In turn, the outermost limit shell will be only crossed by all the unbound shells interior to it, so

$$\begin{aligned} E(r(R_{\star out})) &= E(R_{\star out}) + 8\pi \int dr_{j,out} \frac{\rho(r_j) r_j^2}{r_{\times out}(r_j)} \\ &\equiv E(R_{\star out}) + 2 \frac{\Delta M_{out}}{\langle r_{\times out} \rangle (R_{\star out})}, \end{aligned} \quad (45)$$

where  $\Delta M_{out}$  is the positive mass loss of the outermost limit shell and  $\langle r_{\times} \rangle$  is a reduced crossing radius. Note that, by construction,  $M_{out} > M(R_{\star out}, t \rightarrow \infty) = M_{out} - \Delta M_{out} > 0$ .

Now, supposing the density distribution remains finite we can decompose the crossing of the outermost limit shell by all escaping inner shells into a series of infinitesimal shell crossings. Thus following Eq. (31) we get

$$\begin{aligned} d[E - E_{lim}] &= -8\pi dr_{j,out} \rho(r_{j,out}) r_{j,out}^2 \\ &\times \left( \frac{1}{r_{lim}(M_{\star out}(t_{\times j}))} - \frac{1}{r_{\times out}(r_{j,out})} \right). \end{aligned} \quad (46)$$

As all shells cross outwards<sup>20</sup> and

$$\frac{1}{\langle r_{\times out} \rangle (R_{\star out})} > \frac{1}{r_{lim}(\langle r_{\times out} \rangle)} \geq \frac{1}{r_{lim}(R_{\star out})}, \quad (47)$$

<sup>20</sup> Note that  $R_{\star out}$  starts as a marginally bound shell well inside its limit radius.



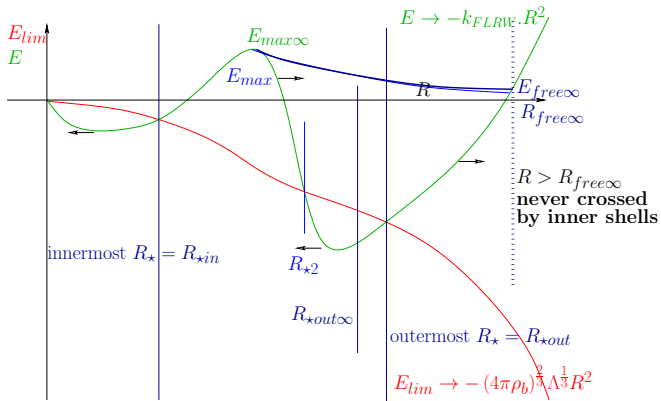


Figure 10. Illustration, on an open background with arbitrary central mass distribution, of the effect of shell crossing on the outer global limit shell previously defined as the outer shell with same energy function as the inner shells' maximum. The time variations of the inner shells' maximum energy function from shell crossings lead to defining it as the outer shell with same energy as the time infinity inner shells' maximum energy function  $E$ : this is shown with the highest of extrapolated time infinity  $E$ s of inner shells' peaks. The global outer limit shell is then just shifted inwards, compared with the integrable analysis.

then, in this case, we have

$$\Delta[E - E_{lim}]_{out} = 2\Delta M_{out} \left[ \frac{1}{\langle r_{\times out} \rangle (R_{\star out})} - \frac{1}{r_{lim}(R_{\star out})} \right] > 0. \quad (48)$$

Thus, the outermost limit shell will shift relatively inwards, following the qualitative analysis of Fig. 6.

Finally, the maximum  $E$  shell initially inside  $R_{\star out}$ , or with horizontal tangent (its initial radius is  $R_{max}$ ), will be only crossed inwards by all the shells starting with radii above it and having an  $E$  below  $E(R_{max}, t \rightarrow \infty)$ , at the moment of crossing. This shell will then follow

$$\Delta[E - E_{lim}]_{max} < 2\Delta M_{max} \times \left[ \frac{1}{r_{lim}(R_{max})} - \frac{1}{\max[r_{\times max}(r_j)]} \right] < 0, \quad (49)$$

similarly as for the innermost limit shell.

We summarize the main result of this section as:

**Result 5.** Consider a  $\Lambda$ -LTB spacetime where shell crossing exists. Then the metric and extrinsic curvature are discontinuous and the discontinuity in  $E$  is given by (29). Furthermore, at  $R_{\star out}$ ,  $\Delta[E - E_{lim}]_{out} > 0$  and, at  $R_{max}$ ,  $\Delta[E - E_{lim}]_{max} < 0$ .

#### 4. Qualitative analysis of limit trapped matter shells

In this section, we argue that the results contained in Summary 1 remain true for the case where  $M$  and  $E$  are not conserved through shell crossing.

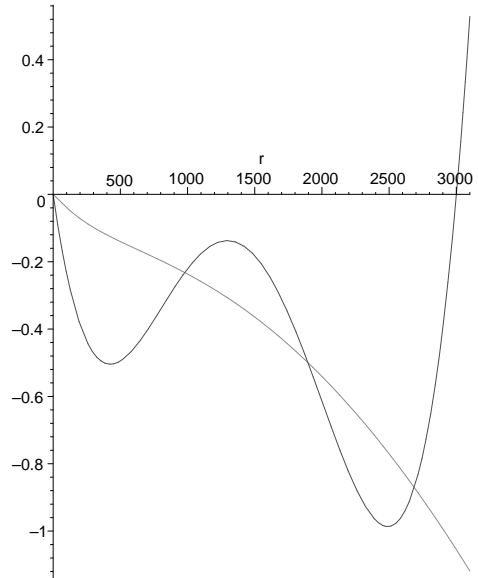


Figure 11. NFW with background  $E_{lim}$  and an example of  $E$  profile given by Eq. (50-54), setting  $R_0 = 3000$ , arbitrarily setting  $x_1 = \frac{1}{4}$ ,  $x_2 = \frac{1}{2}$ ,  $x_3 = \frac{3}{4}$ ,  $\epsilon_1 = 10^{-2}$ ,  $g = 2$  and  $\epsilon = e^{-1}$  so that the figure is proportioned.

We discussed the behaviour of the outermost limit shell  $R_{\star out}$  and of the outward escaping highest energy inner shell  $R_{max}$  in Sec. III D 3. As those determine the two separating shells  $R_{t\star out\infty}$  and  $R_{free\infty}$  studied above, their modifications by shell crossing will indicate that the effective limit shells are just displaced but obey the same general properties. We illustrate this on the open background example (Fig. 8), for which we separated the study of each limit shell.

In Fig.9, we represent the construction of the outer trapper matter shell, using the qualitative evolution of  $R_{\star out}$  and its neighbouring shells from Eq. 48.

In Fig.10, using the qualitative evolution of  $E_{max}$  and its neighbouring shells from Eq. 49, we represent the construction of the inner trapper matter shell for open initial conditions. The subsequent modifications proceed from those qualitative changes and do not modify the formulations of the results from their counterparts in the model where both  $E$  and  $M$  are conserved between shell crossings.

In the case where  $E$  and  $M$  are not conserved, the effect of shell crossing on  $R_{\star out}$  given by Eq. (48) implies only that  $R_{t\star out\infty} < R_{t\star out}$  without qualitative changes and the Definition 3 is verified. In turn, the effect of shell crossing on  $R_{free}$  depends on the effect on  $E_{free}$  from Eq. (49) and by the monotonous increase of  $E$  near infinity and only implies that  $R_{free\infty} < R_{free}$ .

Therefore, the findings of Sec. III D 2, extending the analysis of [5] in the context of shell crossing, are only quantitatively modified as full shell crossing effects only displace inwards both the inner and outer limit trapped matter shells: the initial outermost intersection of  $E$  and  $E_{lim}$  gets unbound and the system at infinity gets con-



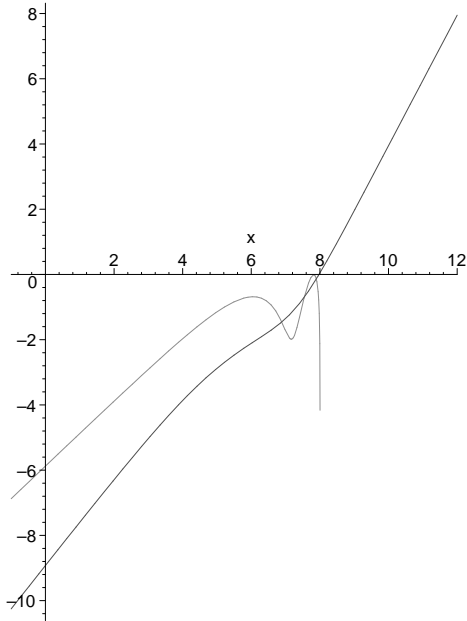


Figure 12. NFW with background  $E_{lim}$  and an example of  $E$  profile given by Eq. (50-54) in  $\log(-E)$ - $\log(-R)$  scale.

sequently reduced in Lagrangian initial radius. In turn, the maximum energy of the inner regions gets lowered, so the inner limit trapped matter surface is also drawn inwards. This displacement modifies only marginally the conclusions obtained in Sec. III D 2, namely: (i) the splitting of the local trapped matter shell is maintained when those shells exist. (ii) Open, flat and closed models with *existing*  $R_{t \rightarrow out}$  (with  $k_{FLRW} < (4\pi\rho_b)^{\frac{2}{3}} \Lambda^{\frac{1}{3}}$ ) all retain an

$R_{t \rightarrow out \infty}$  and (iii) the modification of the maximum energy of the inner regions allows just more asymptotic cosmological flat models to keep their inner limit trapped matter shell, if the shift from  $E_{max}$  tends to  $E_{max \infty} < 0$ .

Therefore, from the sufficient conditions for inner and outer limit trapped matter shells (Res. 4 and 3), the results contained in Summary 1 remain true in the case where  $M$  and  $E$  are not conserved through shell crossing.

#### IV. EXAMPLES: NFW PROFILES WITH ONE UNDERCOMING INTERSECTION

In [5], we studied examples of trapped matter shells using cosmological models with a Navarro, Frenk and White (NFW) density profile [31] and a simple parabolic  $E$  profile. Here we adapt those profiles in order to present one intersection with  $E_{lim}$  of the undercoming type as in the local configuration of Fig. 3, and thus ensure, at the local level, the appearance of shell crossing.

To do so, we use a fourth order polynomial in the canonical Lagrange form, to provide for the behaviour in the intersecting region, that we cut off with an exponential so that an open FLRW term dominates at infinity. We chose the profile to be 0 at the origin and at a characteristic radius  $R_0$  set near the last possible intersection point with the NFW  $E_{lim}$  given by Eq. (4.21) of [5],

$$R_0 \leq R_{-1, E_{lim}}(R_{-1}) = -1,$$

so as to secure the crossings in the physical region. The remaining three points of interpolation are chosen to be set alternately below and above the  $E_{lim}$  curve inside the region set by 0 and  $R_0$ . The form is set by

$$E(R) = \left\{ m_1 \frac{x}{x_1} \frac{x-x_2}{x_1-x_2} \frac{x-x_3}{x_1-x_3} \frac{x-1}{x_1-1} + m_2 \frac{x}{x_2} \frac{x-x_1}{x_2-x_1} \frac{x-x_3}{x_2-x_3} \frac{x-1}{x_2-1} + m_3 \frac{x}{x_3} \frac{x-x_1}{x_3-x_1} \frac{x-x_2}{x_3-x_2} \frac{x-1}{x_3-1} + \epsilon_1 x \right\} e^{-x} - k_\infty R^2 \frac{\epsilon_0 x^2}{(x^2-1)\epsilon_0+1}, \quad (50)$$

where  $x = R/R_0$ , we have denoted the three intermediate points as  $x_1$ ,  $x_2$  and  $x_3$ , the values of the polynomial at those points by  $m_1$ ,  $m_2$  and  $m_3$ ,  $\epsilon_1$  is a small constant making sure we have the freedom to fit  $E(R_0) = E(0) = 0$  where the polynomial itself is built to vanish,  $\epsilon_0$  is a

small constant making sure the polynomial dominates in the interesting range but allowing the curvature at radial infinity to be set by a Friedmann-type  $k_\infty$ . The form (50) automatically vanishes at 0. We chose the polynomial values such that at those points,  $E$  is alternately below,

above and again below  $E_{lim}$ , the last one making sure it remains above -1:

$$E(R_0) = 0 = \epsilon_1 e^{-1} - k_\infty R_0^2 \epsilon_0, \quad \Rightarrow \epsilon_0 = \frac{\epsilon_1}{k_\infty R_0^2 e}, \quad (51)$$

$$\begin{aligned} E(R_1) &= g E_{lim}(R_1) = (m_1 + \epsilon_1 x_1) e^{-x_1} - k_\infty R_0^2 \frac{\epsilon_0 x_1^4}{(x_1^2 - 1) \epsilon_0 + 1} \\ &= (m_1 + \epsilon_1 x_1) e^{-x_1} - \frac{\epsilon_1 x_1^4}{e - (1 - x_1^2) \frac{\epsilon_1}{k_\infty R_0^2}} \quad \Rightarrow m_1 = g E_{lim}(R_1) e^{x_1} \\ &\quad + \epsilon_1 x_1 \left( \frac{x_1^3 e^{x_1}}{e - (1 - x_1^2) \frac{\epsilon_1}{k_\infty R_0^2}} - 1 \right), \quad (52) \end{aligned}$$

$$\begin{aligned} E(R_2) &= \frac{E_{lim}(R_2)}{g} = (m_2 + \epsilon_1 x_2) e^{-x_2} - k_\infty R_0^2 \frac{\epsilon_0 x_2^4}{(x_2^2 - 1) \epsilon_0 + 1} \\ &= (m_2 + \epsilon_1 x_2) e^{-x_2} + \frac{\epsilon_1 x_2^4}{e - (1 - x_2^2) \frac{\epsilon_1}{k_\infty R_0^2}} \quad \Rightarrow m_2 = \frac{E_{lim}(R_2)}{g} e^{x_2} \\ &\quad + \epsilon_1 x_2 \left( \frac{x_2^3 e^{x_2}}{e - (1 - x_2^2) \frac{\epsilon_1}{k_\infty R_0^2}} - 1 \right), \quad (53) \end{aligned}$$

$$\begin{aligned} E(R_3) &= E_{lim}(R_3) - (E_{lim}(R_3) + 1)(1 - \epsilon) \\ &= (E_{lim}(R_3) + 1) \epsilon - 1 = (m_3 + \epsilon_1 x_3) e^{-x_3} - k_\infty R_0^2 \frac{\epsilon_0 x_3^4}{(x_3^2 - 1) \epsilon_0 + 1} \\ &= (m_3 + \epsilon_1 x_3) e^{-x_3} + \frac{\epsilon_1 x_3^4}{e - (1 - x_3^2) \frac{\epsilon_1}{k_\infty R_0^2}} \quad \Rightarrow m_3 = [(E_{lim}(R_3) + 1) \epsilon - 1] e^{x_3} \\ &\quad + \epsilon_1 x_3 \left( \frac{x_3^3 e^{x_3}}{e - (1 - x_3^2) \frac{\epsilon_1}{k_\infty R_0^2}} - 1 \right). \quad (54) \end{aligned}$$

We illustrate this in Figs. (11) and (12) after choosing the values of the density profile identical to those in [5]. The cut off leaves the region under  $R_0$  almost unaffected by the Friedmann term, so the value of  $k_\infty$  is not very relevant there but we set it to -1.

We summarize the result of this section as:

**Result 6.** *For NFW density and initial data given by (50-54), the  $\Lambda$ -LTB spacetime has three shells  $R_*$  such that  $E|_{R_*} = E_{lim}|_{R_*}$ . Furthermore, for this data, there is shell crossing and  $R_{*out} - R_{*out\infty} < 0$  and  $R_{free} - R_{free\infty} < 0$ .*

## V. CONCLUSIONS

We have studied the effects of shell crossing on the existence of trapped matter shells in  $\Lambda$ -LTB spacetimes. In particular, we have considered initial conditions such that: (i) our models approach a FLRW solution at radial infinity and have an initial outgoing Hubble-type flow (ii) the shell crossing of dust remains pressureless and the mass of infinitely thin shells remains finite.

We have shown that the local trapped matter shells discussed in Ref. [5] split in two shells: one outer limit trapped matter shell and one inner limit trapped matter shell.

We have established sufficient conditions for the existence of such shells in  $\Lambda$ -LTB spacetimes, in terms of initial data for which shell crossing occurs. Furthermore, we have derived a number of properties for those shells using a qualitative approach inspired in newtonian-like frameworks of cosmological kinematical models, as in [24, 25].

We have also studied the role of shear in these settings and concluded, as in [18], that shear favours the emergence of trapped matter shells.

Finally, we have given concrete examples where shell crossing occurs and the inner and outer limit trapped matter shells emerge, using NFW data.

As potential applications of our models we note that (i) Due to mass conservation and integrability in the absence of shell crossing at the boundary, the background asymptotic conditions remain FLRW over all time. Therefore, this gives an interesting setting to study the extendability of Birkhoff's theorem to cosmological expanding backgrounds; (ii) Extensions of this work to unsmooth distri-

butions of mass should be possible and might give support to current structure formation analyses using the spherical top hat collapse model, in the case of  $\Lambda$ CDM.

## ACKNOWLEDGMENTS

The work of MLeD is supported by CSIC (Spain) under the contract JAEDoc072, with partial support from CICYT project FPA2006-05807, at the IFT, Universidad Autonoma de Madrid, Spain. Financial support from the Portuguese Foundation for Science and Technology (FCT) under contract PTDC/FIS/102742/2008 and contract CERN/FP/109381/2009 is gratefully acknowledged by J. P. M.. F. C. M. is supported by CMAT, Univ. Minho, through FCT plurianual funding, Project No. PTDC/MAT/108921/2008 and CERN/FP/116377/2010 and Grant No. SFRH/BSAB/967/2010.

## Appendix A: Time infinity definitions

**Definition 5.** *The inner or non-bound shells of initial conditions in  $E$  and  $E_{lim}$ , in the limit  $t \rightarrow \infty$ , induce a few remarkable features defined as follows:*

- $R_{*\infty} \equiv R_{*i}(t \rightarrow \infty)$  is the intersections number  $i$  between  $E(t \rightarrow \infty) = E_{lim}(t \rightarrow \infty)$  taken at time infinity but singled out by its radius in the initial profile of  $E$ ; in particular we note  $R_{*out\infty} \equiv R_{*n}(t \rightarrow \infty)$  for the outermost intersection and  $R_{t*out\infty} \equiv R_{*out\infty}$  when we add the condition  $(E'(t \rightarrow \infty) > E'_{lim}(t \rightarrow \infty))$
- We will note  $E_{max\infty}$  the maximum value taken at time infinity, but singled out in the initial profile, of non-bound  $E$  in the set of shells inside  $R_{*out\infty}$  or outside but with initial horizontal tangent, i.e.  $E_{max\infty} = \{E, \max(E(t \rightarrow \infty)) \wedge ((E' = 0) \vee (0 < R \leq R_{*out\infty})) \wedge (E \geq E_{lim})\}$
- $R_{max\infty}$  is the largest value for which  $E = E_{max\infty}$ , i.e.  $R_{max\infty} = \max\{R, E(R) = E_{max\infty}\}$
- $R_{free\infty}$ , if it exists, is the furthest shell outside  $R_{*out\infty}$  with an increasing  $E$  at  $E = E_{max\infty}$ , i.e.  $R_{free\infty} = \max\{R, (R \geq R_{*out\infty}) \wedge (E = E_{max\infty}) \wedge (E'(R) > 0)\}$
- We will note  $E_{free\infty}$  the value of  $E$ , if it exists, such as  $E_{free\infty} = E(T = 0, R_{free\infty})$ .

## Appendix B: Gauge invariant definitions for inner limit trapped matter shells

We can rewrite  $E$  in terms of gauge invariant quantities with Eqs. (9, 8, 14, 12 and 11)

$$\begin{aligned} \mathcal{L}_n \left( \frac{\Theta}{3} + a \right) &\equiv \left( \frac{\dot{r}}{r} \right)' = \frac{1}{r^2} \left( \frac{r_{lim}}{r} E_{lim} - E \right) \\ \Leftrightarrow E(R) &= \frac{r_{lim}}{R} E_{lim} - R^2 \mathcal{L}_n \left( \frac{\Theta}{3} + a \right) \\ &= r^2 \left( \frac{E_{lim} r_{lim}}{r^3} - \mathcal{L}_n \left( \frac{\Theta}{3} + a \right) \right), \end{aligned}$$

so the condition of existence for  $E_{max}$ , that  $E \geq E_{lim}$ , translates into initial condition with the inequality

$$\begin{aligned} \mathcal{L}_n \left( \frac{\Theta}{3} + a \right) &= \frac{\left( \frac{r_{lim}}{R} - 1 \right) E_{lim}}{R^2} + \frac{1}{R^2} (E_{lim} - E) \\ &\leq \frac{\left( \frac{r_{lim}}{R} - 1 \right) E_{lim}}{R^2} < 0, \end{aligned}$$

or at time infinity into

$$\mathcal{L}_n \left( \frac{\Theta}{3} + a \right) \Big|_{(t \rightarrow \infty)} \leq \frac{\left( \frac{r_{lim}}{r} - 1 \right) E_{lim}}{r^2} \Big|_{(t \rightarrow \infty)} < 0.$$

We get then  $R_{max}$  and  $E_{max}$  from

$$\begin{aligned} R_{max} &= \max \left\{ R, \frac{E}{R^2} = - \min \left\{ \mathcal{L}_n \left( \frac{\Theta}{3} + a \right) \right. \right. \\ &\quad \left. \left. - \frac{E_{lim} r_{lim}}{R^3} \right\} \wedge ((E' = 0) \vee (0 < R \leq R_{*out})) \wedge \left( \mathcal{L}_n \left( \frac{\Theta}{3} + a \right) \right. \right. \\ &\quad \left. \left. \leq \frac{\left( \frac{r_{lim}}{R} - 1 \right) E_{lim}}{R^2} < 0 \right) \right\} \\ \Rightarrow E_{max} &= -R_{max}^2 \min \left\{ \mathcal{L}_n \left( \frac{\Theta}{3} + a \right) - \frac{E_{lim} r_{lim}}{R^3} \right\} \\ &= \max \left\{ R^2 \left( \frac{E_{lim} r_{lim}}{R^3} - \mathcal{L}_n \left( \frac{\Theta}{3} + a \right) \right), \right. \\ &\quad \left. ((E' = 0) \vee (0 < R \leq R_{*out})) \right. \\ &\quad \left. \wedge \left( \mathcal{L}_n \left( \frac{\Theta}{3} + a \right) \leq \frac{\left( \frac{r_{lim}}{R} - 1 \right) E_{lim}}{R^2} < 0 \right) \right\}. \end{aligned}$$

Taken at  $t \rightarrow \infty$ , this translates into

$$\begin{aligned} R_{max\infty} &= \max \left\{ R, E = \max \left\{ -r^2 \left( \mathcal{L}_n \left( \frac{\Theta}{3} + a \right) \right. \right. \right. \\ &\quad \left. \left. - \frac{E_{lim} r_{lim}}{R^3} \right) \right\} \Big|_{(t \rightarrow \infty)} \right\} \wedge ((E' = 0) \vee (0 < R \leq R_{*out\infty})) \\ &\quad \wedge \left( \mathcal{L}_n \left( \frac{\Theta}{3} + a \right) \leq \frac{\left( \frac{r_{lim}}{r} - 1 \right) E_{lim}}{r^2} < 0 \right) \Big|_{(t \rightarrow \infty)} \right\} \end{aligned}$$

$$\Rightarrow E_{max\infty} = \max \left\{ r^2 \left( \frac{E_{lim} r_{lim}}{r^3} - \mathcal{L}_n \left( \frac{\Theta}{3} + a \right) \right) \right\}_{(t \rightarrow \infty)},$$

**Definition 6.** Suppose that  $E_{max\infty}$  defined as

$$E_{max\infty} = \max \left\{ r^2 \left( \frac{E_{lim} r_{lim}}{r^3} - \mathcal{L}_n \left( \frac{\Theta}{3} + a \right) \right) \right\}_{(t \rightarrow \infty)},$$

$$\left( (E' = 0) \vee (0 < R \leq R_{*out\infty}) \right)$$

$$\wedge \left( \mathcal{L}_n \left( \frac{\Theta}{3} + a \right) \leq \frac{\left( \frac{r_{lim}}{r} - 1 \right) E_{lim}}{r^2} < 0 \right) \Big|_{(t \rightarrow \infty)}, \quad (B1)$$

exists. Then, inner limit trapped matter shells are defined, in the models considered with GLTB coordinates, as the locus  $R_{free\infty}$  such that

$$\left( (E' = 0) \vee (0 < R \leq R_{*out\infty}) \right)$$

$$\wedge \left( \mathcal{L}_n \left( \frac{\Theta}{3} + a \right) \leq \frac{\left( \frac{r_{lim}}{r} - 1 \right) E_{lim}}{r^2} < 0 \right) \Big|_{(t \rightarrow \infty)}.$$

$$R_{free\infty} = \max \left\{ R, (R \geq R_{*out\infty}) \right.$$

$$\wedge \left( \frac{\Theta}{3} + a = \sqrt{\frac{E_{max\infty}}{r^2} + 2\frac{M}{r^3} + \frac{1}{3}\Lambda} \right)_{t \rightarrow \infty}$$

$$\left. \wedge (E'(t \rightarrow \infty, R) > 0) \right\}. \quad (B2)$$

Thus, Def. 4 can be rewritten as

- 
- [1] F. Bernardeau, S. Colombi, E. Gaztanaga and R. Scoccimarro, Phys. Rept. **367** (2002) 1 [arXiv:astro-ph/0112551].
- [2] D. F. Mota and C. van de Bruck, Astron. Astrophys. **421** (2004) 71 [arXiv:astro-ph/0401504].
- [3] M. Le Delliou, JCAP, **0601** (2006) 021 [arXiv:astro-ph/0506200].
- [4] I. Maor, Int. J. Theor. Phys. **46** (2007) 2274 [arXiv:astro-ph/0602441].
- [5] J. P. Mimoso, M. Le Delliou & F. C. Mena, Phys. Rev. D **81** (2010) 123514 arXiv:0910.5755 [gr-qc].
- [6] C. Hellaby & K. Lake, Astrophysical Journal **290** (1985) 381-387
- [7] A. Meszaros, MNRAS, **253** (1991) 619
- [8] R. Sussman, Class. Quantum Grav. **27** (2010) 175001.
- [9] R. A. Sussman & G. Izquierdo, *A dynamical systems study of the inhomogeneous Lambda-CDM model*, preprint arXiv:1004.0773
- [10] S. M. C. Goncalves, Phys. Rev. D **63** (2001) 124017 [arXiv:gr-qc/0107087].
- [11] K. Bolejko, A. Krasinski & C. Hellaby, MNRAS **362** (2005) 213
- [12] R. P. A. C. Newman, Class. Quantum Grav. **3** (1986) 527
- [13] B.C. Nolan, Class. Quant. Grav. **20** (2003) 575 [arXiv:gr-qc/0301028].
- [14] D. Nunez, H. P. de Oliveira and J. Salim, Class. Quant. Grav. **10** (1993) 1117 [arXiv:gr-qc/9302003].
- [15] S. M. C. Goncalves, Phys. Rev. D **66** (2002) 084021 [arXiv:gr-qc/0212124].
- [16] P. D. Lasky, & A. W. C. Lun, Phys. Rev. D **74** (2006) 084013
- [17] C. W. Misner and D. H. Sharp, Phys. Rev. B **136**, 571 (1964).
- [18] A. Di Prisco, L. Herrera, E. Fuenmayor and V. Varela, Phys. Lett. A **195** (1994) 23; A. Abreu, H. Hernandez, and L. A. Nunez, Classical Quantum Gravity **24** (2007) 4631; A. Di Prisco, L. Herrera, and V. Varela, Gen. Relativ. Gravit. **29** (1997) 1239; L. Herrera and N. O. Santos, Phys. Rep. **286** (1997) 53.
- [19] S. S. Deshingkar, S. Jhingan, A. Chamorro & P. S. Joshi, Phys. Rev. D **63** (2001) 124005
- [20] S. M. C. Goncalves, Phys. Rev. D **63** (2001) 064017
- [21] F. C. Mena, B. Nolan and R. Tavakol, Phys. Rev. D, **70** (2004) 084030
- [22] Y. B. Zeldovich & L. P. Grishchuk, MNRAS **207** (1984) 23
- [23] K. Lake, Phys. Rev D **29** (1984) 1861
- [24] S. F. Shandarin, & Ya. B. Zel'Dovich, Rev.Mod.Phys. **61**, (1989) 185
- [25] P. Sikivie, I. I. Tkachev, & Y. Wang, Phys.Rev.D, **56** (1997) 1863
- [26] P. Sikivie, Phys. Rev. D **60** (1999) 063501 [arXiv:astro-ph/9902210].
- [27] L. D. Landau, & E. M. Lifshitz, *The Classical Theory of Fields* (New York: Pergamon, 1975).
- [28] C. Hellaby & K. Lake, Astrophysical Journal **282** (1984) 1-10.
- [29] M. Le Delliou, 2001, PhD Thesis, Queen's University, Kingston, Canada.
- [30] M. Le Delliou, A.&A **490** (2008) L43 [arXiv: 0705.1144].
- [31] J. F. Navarro, C. S. Frenk and S. D. M. White, Astrophys. J. **462** (1996) 563.